High Gain WAT Antenna for 38 GHz 5G Systems

Rafał Przesmycki and Marek Bugaj

Military University of Technology, Warsaw, Poland

https://doi.org/10.26636/jtit.2023.4.1386

Abstract — The article presents a high gain WAT microstrip antenna designed for 5G communication systems operating in the 38 GHz band. The antenna concerned has a compact structure with dimensions of 5.16×5.05 mm. Rogers RT5880 laminate with a dielectric coefficient of 2.2 and a thickness of 0.254 mm was used as its substrate. The antenna works at a center frequency of 38 GHz and is characterized by a low reflection coefficient of –29.11 dB, a high energy gain of 7.61 dB and a wide operating band of 1.21 GHz (3.18%). The paper presents an analysis of the simulation results and measurements of the device's electrical parameters and radiation patterns.

Keywords — microstrip antenna, high gain, 5G wireless system

1. Introduction

5G is a new telecommunications standard expected to enable a fifty-fold or higher increase in transmission speeds, compared to 4G networks currently in use. 5G networks are intended, inter alia, to accelerate the development of the Internet of Things, telemedicine services, autonomous vehicles, and smart cities [1]. One of the key conditions for the implementation of 5G is to ensure relevant frequency resources. It is also necessary to implement the so-called "dense networks", i.e. networks using a high number of short-range base stations to significantly increase spectral efficiency and, consequently, the throughput offered to the customer. 5G networks move away from large cell-based solutions, replacing them with networks consisting of numerous small cells [2]–[4].

The 5G network technology allows to rely on several frequencies bands. In accordance with the current 5G standardization and spectrum availability status, the use of three bands is expected: low-band 700 MHz (694–790 MHz), mid-band 3.6 GHz (3.4–3.8 GHz), as well as high-band 26 GHz (24.25–27.5 GHz) and 38 GHz (37 GHz–40 GHz), with the maximum frequency resources available in these bands being 2×30 MHz (part of the band), 400 MHz, and 3250 MHz, respectively. Such an approach allows the users of mobile terminals to access 5G network services in many countries. Mature 5G networks will use many bands simultaneously, including bands currently used by 4G systems (1800 MHz, 2100 MHz, 2600 MHz) [2], [5], [6].

The 700 MHz band (694–790 MHz) allows to communicate within the range of up to several kilometers from the base station – a distance that is longer than in the case of 4G, due to good penetration of radio signal inside buildings. Therefore, this band is known as "coverage" or "range" band and is suitable for non-urban areas, with a relatively low density of 5G network users. The 60 MHz-wide frequency spectrum limits network throughput which may be comparable to that known from 4G, or may even be slightly lower [7]–[9].

The 3.6 GHz band (3.4–3.8 GHz) enables a communication range of up to few kilometers from the base station and is characterized by poor radio signal penetration inside buildings. However, unlike the 700 MHz band, the larger frequency resources allow for high throughputs, up to 10 times higher than in 4G. Therefore, this band is known as "capacitive" and provides the parameters required to operate multiple connected devices simultaneously. In addition, this band (with some limitations) has been available for a long time now and is successfully relied upon to build 5G networks in dense environments. An additional advantage of 5G networks operating in this band is the introduction of very low data transmission delays (a few milliseconds), which is important for supporting Internet of Things devices [7]–[9].

The 26 GHz and 38 GHz bands (with the former used in Europe and the latter in China and the USA) cover the frequency ranges of 24.25 to 27.5 GHz and 37 to 40 GHz, respectively. This enables the distribution of a maximum of four 200 MHz channels in the 26.5–27.3 GHz range and two 400 MHz channels in the 37.5–37.8 GHz range. Communication bands will enable high throughputs with low transmission delays for mobile terminals at distances of up to 500 m. Therefore, the plans assume that they will be used mainly for IoT and fixed connections and are therefore referred to as "radio fiber optic" [7]–[9].

In addition to providing faster connections and greater capacity, 5G networks offer another very important benefit, namely fast response time, also known as latency. Latency is the time it takes for devices to respond to each other within a wireless network. The typical response time for a 3G network was 100 ms, for a 4G network it is approximately 30 ms, while in a 5G network, it has been reduced to as little as 1 ms [5]–[7]. To meet such specific requirements, 5G networks use a large number of small cells located closer to the individual users and devices to ensure good performance. Hence, a significant number of antennas will be installed indoors, especially in public buildings, sports centers, as well as at railway stations and shopping malls. It should be emphasized that such aerials installed close to people will be smaller than those currently used in microcell base stations. In a traditional antenna system, power is radiated over a wide angle, to cover

the entire service area, while in an active 5G antenna relying on massive MIMO technology, power is radiated in specific directions and is focused on one user or group located in the service area. The direction of radiation automatically focuses on moving users to improve link efficiency and to mitigate interference [7]–[9].

In the uplink direction, the cell's coverage may be significantly improved by using multi-antenna systems for lower band uplinks, when high band coverage drops to a low level, e.g. when rain causes high environmental attenuation at higher frequencies. Therefore, cell coverage can be improved in the uplink direction by switching to a lower band or by using antennas with a higher energy gain [9].

In such a context, the article presents a small (10×10 mm) microstrip antenna intended for operation in 38 GHz high band 5G systems with high gain. The design has been simulated, fabricated, and measured to verify its electrical parameters.

2. Antenna Model

The main assumption for the designed antenna is that it will be operating in a 5G high band range of 38 GHz. The remaining important requirements include the following: small dimensions of the antenna (not larger than 10×10 mm), the highest possible energy gain, linear polarization, and the type of substrate material from which the antenna is to be made. Professional type Rogers RT5880 laminate was chosen for prototype fabrication with a thickness of $h = 0.254$ mm, electrical permittivity of $\varepsilon_r = 2.2$ and low losses of $\mathrm{tg}\,\delta = 0.0009$. It consists of 3 layers, where the middle part is made of aluminum oxide and the outer layers are filled with a glass-epoxy resin. Such an arrangement ensures high durability, moisture resistance, and ease of processing, which makes it a popular choice for microstrip antennas.

Designing a microstrip antenna is a complex process that involves many steps and calculations. The process of determining the parameters of a microstrip antenna with a rectangular radiator begins by determining its dimensions. To determine the size of the radiator, the following equation is used [10]–[13]:

$$W = \frac{c}{2f_r}\sqrt{\frac{2}{\varepsilon_r + 1}} = 3.12 \text{ mm}\,, \tag{1}$$

where W is patch width, f_r is resonant frequency, i.e. 38 GHz, c is the speed of light, and ε_r is the dielectric constant.

The next step is to determine the length of the radiating element. First, the effective electrical permittivity ε_{reff} of the substrate must be calculated [10]–[12]:

$$\varepsilon_{reff} = \frac{\varepsilon_r + 1}{2} + \frac{\varepsilon_r - 1}{2\sqrt{1 + 12\dfrac{h}{W}}} = 2.03\,, \tag{2}$$

where h is substrate thickness.

After calculating ε_{reff}, the effective length of radiator L_e should be determined from [10]–[12]:

$$L_e = \frac{c}{2f_r\sqrt{\varepsilon_{reff}}} = 2.77 \text{ mm}\,. \tag{3}$$

The shortening of the length of the radiating patch is calculated as [10]–[12]:

$$\Delta L = \frac{0.412\,h\left(\varepsilon_{reff} + 0.3\right)\left(\dfrac{W}{h} + 0.264\right)}{\left(\varepsilon_{reff} - 0.258\right)\left(\dfrac{W}{h} + 0.8\right)} = 0.013 \text{ mm}\,. \tag{4}$$

The final length of the radiating element is:

$$L = L_e - 2\Delta L = 2.74 \text{ mm}\,. \tag{5}$$

After performing the above calculations, the minimum size of the ground plane should be estimated. The rule of thumb is that the size of the ground plane should be larger than the radiating element (at least by six times the substrate thickness) in both directions [10]–[12]:

$$L_s = L + 6h = 4.264 \text{ mm}\,, \tag{6}$$

$$W_s = W + 6h = 4.644 \text{ mm}\,. \tag{7}$$

For initial design, the values from Eqs. (6)-(7) determining the size of the ground plane were multiplied by 2.5, i.e., to 10.66 mm and 11.61 mm, respectively.

The last step in the antenna design process is to determine the size of the feed line. For a characteristic impedance of Z_C = 50 Ω, the process starts with the calculation of auxiliary variables a and b:

$$\begin{aligned} a &= \frac{Z_C}{60}\sqrt{\frac{\varepsilon_r + 1}{2}} + \frac{\varepsilon_r - 1}{\varepsilon_r + 1}\left(0.23 + \frac{0.11}{\varepsilon_r}\right) = 1.159\,, \\ b &= \frac{60\pi^2}{Z_C\sqrt{\varepsilon_r}} = 7.976\,. \end{aligned} \tag{8}$$

Because a is greater than 1.52, the width and the minimum length of the power line are determined from [10]–[12]:

$$\begin{aligned} W_f &= \frac{2}{\pi}\left\{b - 1 - \ln\left(2b - 1\right) + \frac{\varepsilon_r - 1}{2\varepsilon_r}\right. \\ &\left.\cdot\left[\ln\left(b - 1\right) + 0.39 - \frac{0.61}{\varepsilon_r}\right]\right\}\cdot h = 0.25 \text{ mm}\,, \\ L_f &= 3 \cdot h = 0.762 \text{ mm}\,. \end{aligned} \tag{9}$$

As a result, a model was obtained with the dimensions presented in Tab. 1. It reflects the preliminary design of the antenna.

For the initial antenna dimension values, a WAT antenna project was created in the CST Microwave Studio software. This tool provides electrical parameters and radiation patterns. Initially, the value of the S_{11} coefficient and energy gain G were taken into account. Figures 4 and 5 show the obtained values of the S_{11} reflection and G energy gain coefficients, as a function of frequency for the preliminary model of the proposed antenna (first iteration). The values obtained are below expectations. The initial model also failed to meet the assumptions regarding the physical size of the antenna. This resulted in a change in the antenna structure to tune the model to the assumed parameters. The changes introduced to the structure are shown in Fig. 1, with the size of the ground plane, the dimensions of the radiating element, and the dimensions of the feed line being modified. Detailed information concerning the subsequent iterations is also presented in Tab. 1. In the course of the optimization process,

Tab. 1. Antenna dimensions for all iterations (in millimeters).

Model		Calculated	Preliminary	WAT	Final
Iteration no.		1	2	3	4
Substrate width	W_s	11.61	10.0	10.0	5.16
Substrate length	L_s	10.66	10.0	10.0	5.05
Ground plane width	W_e	11.61	10.0	10.0	5.16
Ground plane length	L_e	10.66	10.0	10.0	5.05
Patch width	W_p	3.12	3.10	3.10	3.10
Patch length	L_p	2.74	2.09	2.09	2.06
Substrate thickness	h	0.254	0.254	0.254	0.254
Feed line width	W_f	0.25	0.25	0.25	0.107
Feed line length	L_f	3.63	3.63	3.95	4.02
WAT letter height	L_w	-	-	1.00	1.00
WAT letter width	W_w	-	-	0.10	0.10

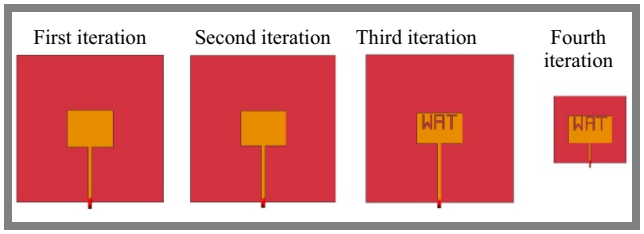

Fig. 1. Antenna designs stages.

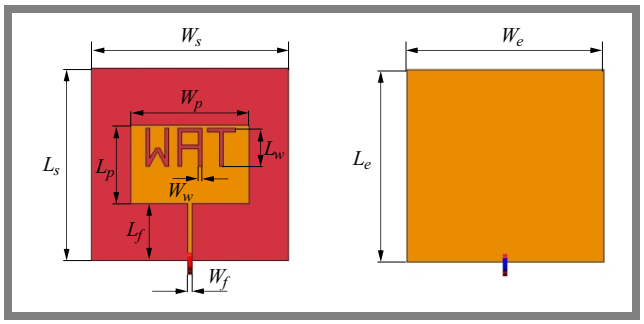

Fig. 2. Microstrip antenna and its dimensions.

the length and width of the antenna, as well as the ground plane (W_s, W_e, L_s, L_e), the length and width of the radiator (L_p, W_p), and the length and width of the feed line (L_f, W_f) were varied. Other structure components, such as thickness and electrical permittivity of the substrate and the size of the WAT letters, have remained unchanged. As a result of the optimization process, the antenna model shown in Fig. 2 was obtained with the dimensions shown in Tab. 1 as those of the "final" model (fourth iteration). To verify the simulations, a physical model of the antenna was fabricated, as shown in Fig. 3. The reflection coefficient S_{11} and energy gain G, as a function of frequency, for the final model of the proposed antenna are shown in Figs. 4 and 5, respectively. For the final model of the proposed antenna, simulations and measurements were carried out to determine the antenna's electrical parameters.

3. Measurements Results

The measurement campaign was conducted using the Rohde & Schwarz ZVA67 network analyzer with the antenna connected using a low-loss, high-frequency cable with a 2.40 mm SMA type connector. Figure 6 shows the lab test bench used during the measurements of electrical parameters, while Fig. 7 shows the test setup during radiation pattern measurements.

Fig. 3. Fabricated final model in relation to an EUR 1 coin.

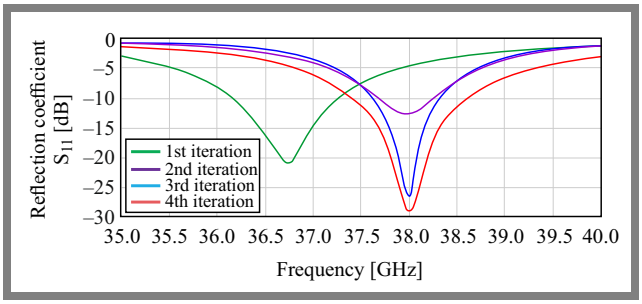

Fig. 4. S_{11} reflection coefficient as a function of frequency for all antenna iterations.

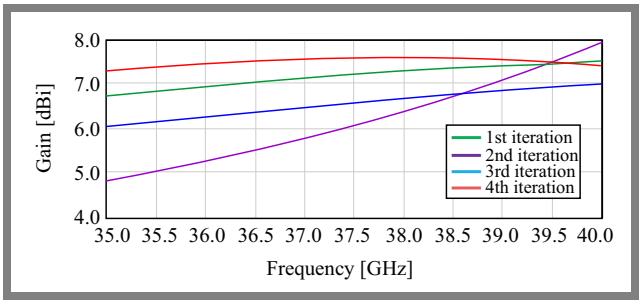

Fig. 5. Energy gain as a function of frequency for four iterations.

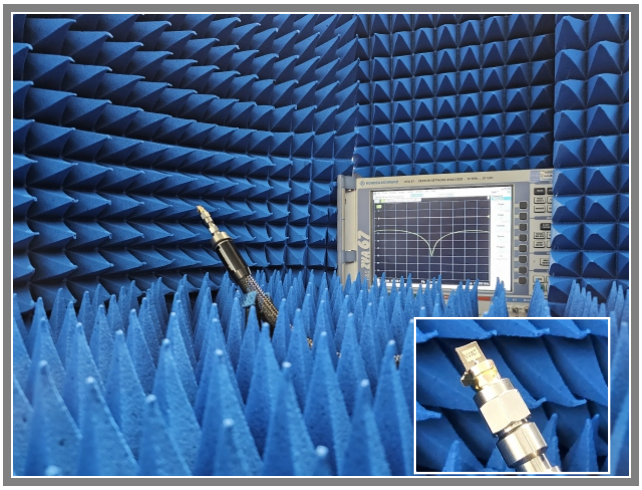

Fig. 6. Setup used for measuring electrical parameters.

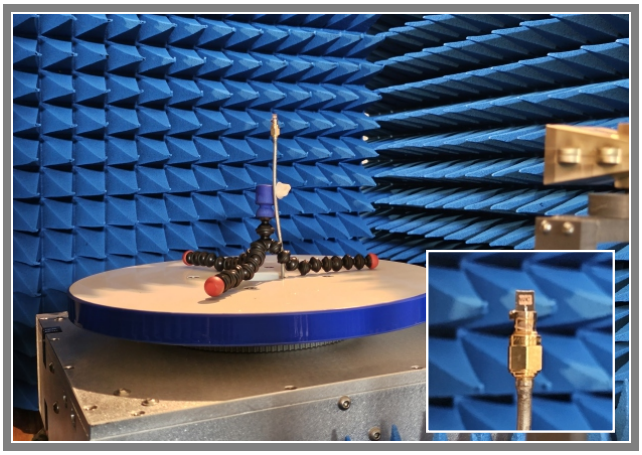

Fig. 7. Measurement of the antenna's radiation patterns.

The obtained reflection coefficient, VSWR, input impedance and energy gain values, as well as current distribution in the antenna and the radiation patterns were compared to analyze the properties of the proposed design.

3.1. Reflectance Coefficient

The S_{11} coefficient determines the operating bandwidth. Figure 8 shows simulation data and measurement results for the proposed WAT model. The antenna's resonance value equals 38 GHz, with a return loss of –29.11 dB. The operating bandwidth is 1.21 GHz, i.e., 3.18%.

3.2. Voltage Standing Wave Ratio (VSWR)

In the case of a patch antenna, the voltage standing wave ratio (VSWR) should not exceed 2 over the entire operating band. As presented in Fig. 9, the VSWR value at the resonance frequency of 38 GHz is 1.07 and the VSWR value of 2 appears at 37.41 GHz and 38.62 GHz, respectively. Thanks to this, the operating bandwidth of the proposed antenna covers all channel widths used in the 38 GHz band, which confirms its suitability for use in 5G systems.

3.3. Input Impedance

In general, the input impedance of the antenna should match the 50 Ω impedance of the feed line. In the proposed model, the width and length of the feed line result in an input impedance of $Z = 46.58 - \text{j}0.24\ \Omega$ at a resonance frequency of 38.0 GHz, and for extreme frequencies of the working band, the input impedance is $Z = 53.26 - \text{j}34.84\ \Omega$ for 37.41 GHz, and $Z = 45.44 + \text{j}31.29\ \Omega$ for 37.62 GHz. De-

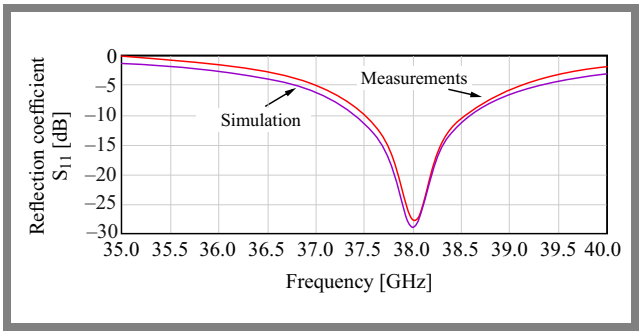

Fig. 8. Final model's S_{11} reflection coefficient as a function of frequency.

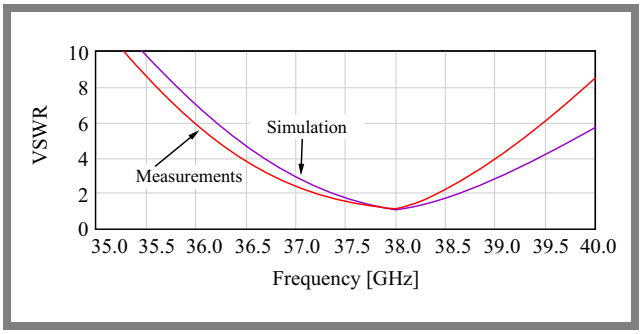

Fig. 9. VSWR for the final model.

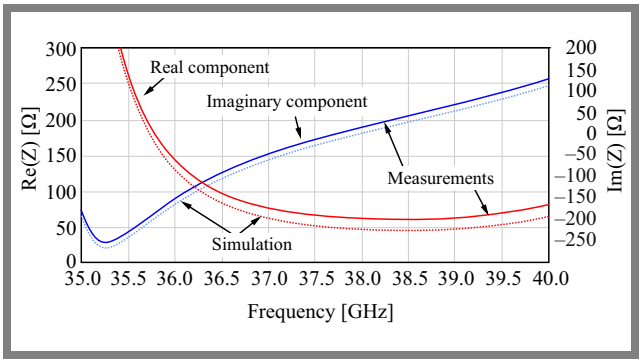

Fig. 10. Input impedance of the final model of the proposed antenna.

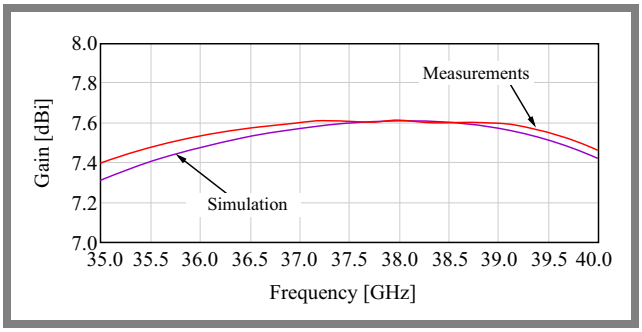

Fig. 11. Energy gain for the final model of the antenna.

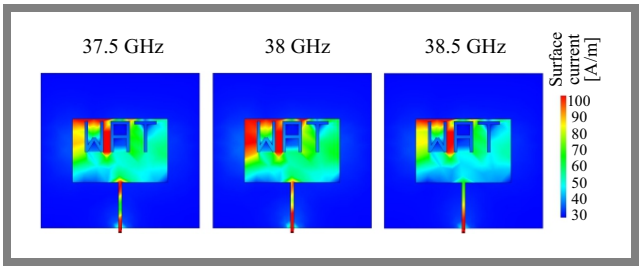

Fig. 12. Current distribution in the designed antenna at 37.5 GHz, 38 GHz, and 38.5 GHz.

Tab. 2. Beamwidth at –3 dB for vertical and horizontal polarization.

Operating frequency [GHz]	Beamwidth at –3 dB [°]	Operating frequency [GHz]	Beamwidth at –3 dB [°]
Vertical polarization		Horizontal polarization	
37.25	76.63	37.25	79.39
37.50	76.19	37.50	79.73
37.75	75.76	37.75	80.12
38.00	75.33	38.00	80.53
38.25	74.91	38.25	80.99
38.50	74.51	38.50	81.50
38.75	74.12	38.75	82.08

tailed input impedance waves for the proposed antenna, as a function of frequency, are shown in Fig. 10.

3.4. Energy Gain

Energy gain is one of the most important parameters taken into account when dealing with antennas, as it should be as high as possible. The energy gain is given in relation to an isotropic antenna and is expressed in dBi. The analyzed model has a gain of 7.61 dBi at 38 GHz. The obtained value is considered to be very good for a single-element microstrip antenna, which is a great achievement for such a small design. This value was achieved thanks to the appropriate shape of the radiator (patch) which has a cutout in the form of a WAT inscription. The energy gain, as a function of frequency, for the designed WAT model is illustrated in Fig. 11.

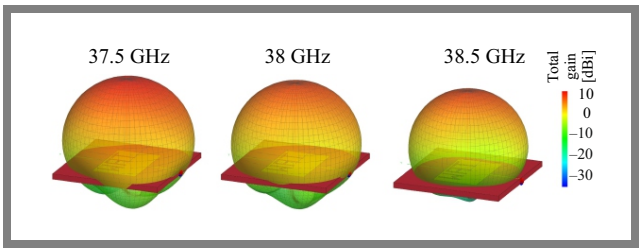

Fig. 13. 3D radiation patterns of the designed antenna for 37.5 GHz, 38 GHz, and 38.5 GHz.

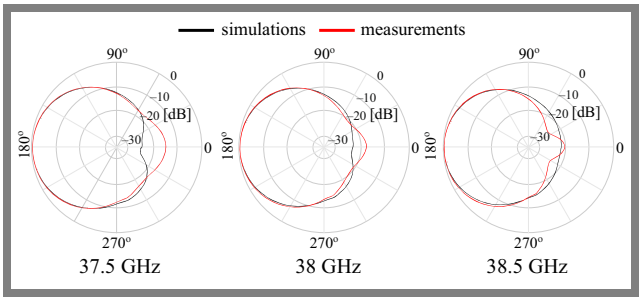

Fig. 14. Normalized radiation pattern of the designed antenna for center and sideband frequencies and vertical polarization.

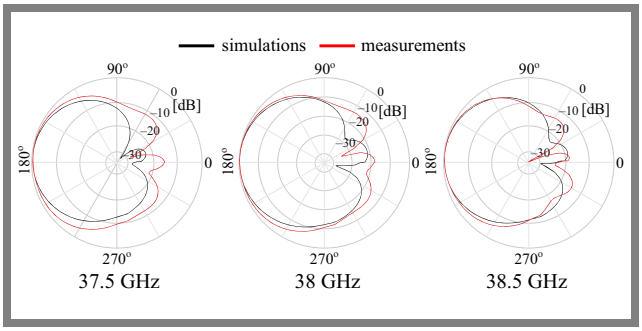

Fig. 15. Normalized radiation pattern of the designed antenna for horizontal polarization.

3.5. Current Distribution

In a microstrip antenna, value of the current at the end of the radiating element i.e., at the edge of the patch, should be minimal. Due to the voltage at the edge of the patch being out of phase with the current, the voltage will peak at the end of the patch, while the current is close to zero. A similar scenario will be experienced halfway along the wavelength i.e., at the beginning of the patch. The proposed antenna confirms the above-mentioned general relationships, as presented in Fig. 12 which illustrates the current distribution of the developed antenna for 37.5 GHz, 38 GHz and 38.5 GHz.

3.6. Radiation Patterns

The radiation pattern illustrates how the antenna radiates energy in space. It represents a normalized distribution of electric field or a relative distribution of surface power density. The graphs are determined along two planes, horizontal and vertical, and can also be presented in a three-dimensional form. Figure 13 shows a 3D version of the simulated radiation patterns of the WAT antenna for 37.5 GHz, 38 GHz, and 38.5 GHz bands, respectively. Figure 14 shows normalized

radiation characteristics of the proposed antenna in the polar coordinate system for vertical polarization, obtained during simulations and measurements, while Fig. 15 shows the normalized radiation characteristics of the proposed antenna in the polar coordinate system for horizontal polarization, obtained during simulations and measurements.
From the presented graphs, one may see that the designed antenna can be effectively used for high speed transmissions in densely populated places.
Based on the presented radiation patterns for vertical polarization for center and sideband frequencies, the –3 dB beamwidth was determined. For vertical polarization, the beamwidth narrows as the frequency increases and is at its narrowest at 38.75 GHz.
For horizontal polarization, beamwidth narrows as well as the frequency increases and is at its narrowest at 38.25 GHz. For both polarizations, the main beamwidth determined for horizontal polarization at the –3 dB level is presented in Tab. 2.

3.7. Cross-polarization Patterns

Co-polarization radiation pattern it is a graph of the desired polarization of the wave to be radiated by the antenna. Cross-polarization is radiation that is orthogonal to the desired polarization of the wave (polarization of the wave from the transmitting antenna).
Figure 16a shows the cross- and co-polarization radiation pattern of the proposed antenna for 37.5 GHz, 38 GHz, and 38.5 GHz in the polar coordinates system for vertical polarization, while Fig. 16b shows the cross- and co-polarization radiation pattern in the polar coordinates system for horizontal polarization of the transmitting antenna, at the same frequencies.

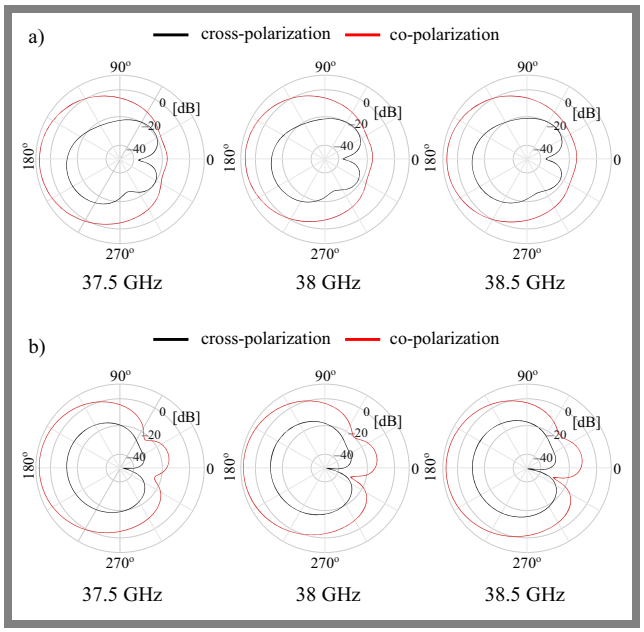

Fig. 16. Cross- and co-polarization radiation pattern of the proposed antenna for center and sideband frequencies in the polar coordinates system for: a) vertical polarization and b) horizontal polarization.

4. Comparison with Other Designs

The parameters of the proposed WAT microstrip antenna, such as energy gain, impedance matching and operating bandwidth, are verified against similar designs to obtain compare their performance. The frequency response of the measured S_{11} parameter for the proposed antenna is not the lowest among the compared antennas presented in [13]–[16]. Nevertheless, it still remains relatively low.
The minimum return loss value for the WAT antenna is –29.11 dB (VSWR ∼1.07), while in [13] it is –40.00 dB, in [14] –41.00 dB, in [15] –34.04 dB, and in [16] it is –24.25 dB. Moreover, for the proposed WAT antenna, the bandwidth (BW) is similar to other antennas and for $S_{11} \leqslant -10$ dB, i.e., VSWR $\leqslant 2$ is 1.21 GHz with the center frequency of 38.00 GHz. For the proposed WAT antenna, the energy gain is the highest (7.61 dBi), while in designs from [13]–[16], the gain equals 6.85, 6.33, 6.80, and 6.98 dBi, respectively.
Table 3 contains a comparative summary of the proposed antenna with the antennas described in papers [13]–[16]. The energy gain value obtained for the WAT antenna is very high for this type of antennas having the form of a single-element radiating element.

5. Conclusions

The article presents an analysis of the simulation results and measurements of the electrical parameters and radiation characteristics of a small microstrip microwave antenna. The proposed designed operates in 5G systems with a center frequency of 38 GHz and is characterized by a low reflection coefficient of –29.11 dB, a very high energy gain of 7.61 dBi, and a bandwidth of 1.21 GHz (3.18%).

References

[1] E. Korzeniowska, A. Krawczyk, E. Łada-Tondyra, and J. Plewako, "Technologia 5G jako Etap Rozwoju Komunikacji Bezprzewodowej", *Przegląd Elektrotechniczny*, vol. 95, no. 12, pp. 144–147, 2019 (https://doi.org/10.15199/48.2019.12.31) [in Polish].
[2] A. Tikhomirov, E. Omelyanchuk, and A. Semenova, "Recommended 5G Frequency Bands Evaluation", in: *2018 Systems of Signals Generating and Processing in the Field of on Board Communications*, Moscow, Russia, 2018 (https://doi.org/10.1109/SOSG.2018.8350639).
[3] M. Benisha, R.T. Prabu, and V.T. Bai, "Requirements and Challenges of 5G Cellular Systems", in: *2016 2nd International Conference on Advances in Electrical, Electronics, Information, Communication and Bio-Informatics (AEEICB)*, Chennai, India, pp. 251–254, 2016 (https://doi.org/10.1109/AEEICB.2016.7538283).
[4] P. Marsch *et al.* (Eds.), *5G System Design: Architectural and Functional Considerations and Long Term Research*, Wiley, 608 p., 2018 (https://doi.org/10.1002/9781119425144).
[5] L.F. Chang, "Journey to 5G", in: *2019 International Symposium on VLSI Technology, Systems and Application (VLSI-TSA)*, Hsinchu, Taiwan, 2019 (https://doi.org/10.1109/VLSI-TSA.2019.8804689).
[6] V. Chauhan and Srinivasans, "A Review on 5G Network System with its Limitation and Different Approaches to Build Strong 5G Network System", in: *2022 3rd International Conference on Intelligent Engineering and Management (ICIEM)*, London, UK, pp. 403–410,

Tab. 3. Comparison of bandwidths achieved in the present work and values shown in other publications.

Performance measure	Proposed WAT antenna	Paper [13]	Paper [14]	Paper [15]	Paper [16]
Center frequency	38.00 GHz	37.96 GHz	38.50 GHz	37.40 GHz	38.00 GHz
S_{11} for center frequency	–29.11 dB	–40.00 dB	–41.00 dB	–34.04 dB	–24.25 dB
BW (VSWR $\leqslant$ 2)	1.21 GHz	2.14 GHz	1.02 GHz	1.40 GHz	0.90 GHz
Relative BW	3.18%	5.63%	2.64%	3.73%	2.36%
Gain	7.61 dBi	6.85 dBi	6.33 dBi	6.80 dBi	6.98 dBi

2022 (https://doi.org/10.1109/ICIEM54221.2022.9853134).

[7] J. Senic *et al.*, "Challenges for 5G and Beyond", in: *2022 16th European Conference on Antennas and Propagation (EuCAP)*, Madrid, Spain, 2022 (https://doi.org/10.23919/EuCAP53622.2022.9769413).

[8] C. Hausl, J. Emmert, M. Mielke, B. Mehlhorn, and C. Rowell, "Mobile Network Testing of 5G NR FR1 and FR2 Networks: Challenges and Solutions", in: *2022 16th European Conference on Antennas and Propagation (EuCAP)*, Madrid, Spain, 2022 (https://doi.org/10.23919/EuCAP53622.2022.9769635).

[9] E.J. Khatib and R. Barco, "Optimization of 5G Networks for Smart Logistics", *Energies*, vol. 14, no. 6, art. no. 1758, 2021 (https://doi.org/10.3390/en14061758).

[10] J.R. James and P.S. Hall, *Handbook of Microstrip Antenna*, London, 856 p., 1989 (https://doi.org/10.1049/PBEW028F).

[11] A.G. Derneryd, "A Theoretical Investigation of the Rectangular Microstrip Antenna Element", *IEEE Transactions on Antennas and Propagation*, vol. 26, no. 4, pp. 532–535, 1978 (https://doi.org/10.1109/TAP.1978.1141890).

[12] W. Ahmad and W.T. Khan, "Small Form Factor Dual Band (28/38 GHz) PIFA Antenna for 5G Applications", in: *IEEE MTT-S International Conference on Microwaves for Intelligent Mobility (ICMIM)*, Nagoya, Japan, pp. 21–24, 2017 (https://doi.org/10.1109/ICMIM.2017.7918846).

[13] A.A.B. Binshitwan, S.M. Keskeso, A.A. Alquzayzi, and A. Elbarsha, "38 GHz Rectangular Microstrip Antenna with DGS for 5G Applications", in: *2021 International Congress of Advanced Technology and Engineering (ICOTEN)*, Taiz, Yemen, 2021 (https://doi.org/10.1109/ICOTEN52080.2021.9493463).

[14] M. El Halaoui, L. Canale, A. Asselman, and G. Zissis, "Dual-Band 28/38 GHz Inverted-F Array Antenna for Fifth Generation Mobile Applications", *Proceedings*, vol. 63, no. 1, art. no. 53, 2020 (https://doi.org/10.3390/proceedings2020063053).

[15] A.E. Farahat and K.F.A. Hussein, "Dual-Band (28/38 GHz) Wideband MIMO Antenna for 5G Mobile Applications", *IEEE Access*, vol. 10, pp. 32213–32223, 2022 (https://doi.org/10.1109/ACCESS.2022.3160724).

[16] S. Agarwal and Prachi, "High Gain Linear 1×4 X-slotted Microstrip Patch Antenna Array for 5G Mobile Technology", *Journal of Telecommunications and Information Technology*, no. 1, pp. 50–55, 2020 (https://doi.org/10.26636/jtit.2020.137319).

Rafał Przesmycki, Ph.D.
Department of Electronics
https://orcid.org/0000-0003-0396-2451
E-mail: rafal.przesmycki@wat.edu.pl
Military University of Technology, Warsaw, Poland
https://www.wat.edu.pl

Marek Bugaj, Ph.D.
Department of Electronics
https://orcid.org/0000-0003-0188-1308
E-mail: marek.bugaj@wat.edu.pl
Military University of Technology, Warsaw, Poland
https://www.wat.edu.pl